Proceedings of the 33rd Chinese Control Conference
July 28-30, 2014, Nanjing, China

Forward and Retraced Scanning Combined Imaging Method for Fast Scanning Atomic Force Microscopy

REN Xiao [1,2], FANG Yongchun [1,2], LV Qing [1,2], and WU Yinan [1,2]

1. Institute of Robotics and Automatic Information System, Nankai University, Tianjin, 300071, China

2. Tianjin Key Laboratory of Intelligent Robotics, Tianjin, 300071, China
E-mail: yfang@robot.nankai.edu.cn

Abstract: For nearly all atomic force microscopies (AFMs) utilized now, only the signals in forward scanning process are employed to reconstruct the sample surface topography, while the retraced scanning process is just for adjustment. In this paper, a forward and retraced scanning combined imaging method for AFM is proposed to increase surface reconstruction accuracy. Specifically, two reconstructed topography images are obtained, one is for forward scanning and the other is for retraced scanning; the hysteresis distortion is compensated with a data fusion based post-processing method; then the two images are combined together with confidence levels to reconstruct the final accurate topography image. This novel imaging method is especially valid for fast scanning tasks, when it is hard to accurately reconstruct the sample surface topography with only forward scanning signals. Some simulation and experimental results are included to demonstrate the superior performance of the proposed imaging method.

Key Words: Atomic Force Microscopy (AFM), Combined Imaging Method, Hysteresis Compensation, Fast Scanning.

1 Introduction

Since its invention, atomic force microscopy (AFM) [1] has brought a great revolution in the domain of nano-science and nano-technology [2]. Attributed to its outstanding advantages such as high resolution and convenience for sample preparation, AFM has been widely used in life science, material engineering, and so on.

For AFM systems, the main bottleneck for further application is the slow scanning speed. In order to supervise some chemical and biological process on-line, high speed scanning is required without much compromise on imaging resolution. The most considered limitations for scanning speed come from the response time of Z-axis control sub-system. In general, there are two main approaches to promote the control effects: a) on the aspect of hardware, a piezo-scanner with high resonant frequency is usually adopted, and some elaborate scanner structures are then designed [3, 4]; b) on the aspect of control/imaging strategy, some more advanced control algorithms [5, 6, 7] and imaging methods [8, 9] are proposed based on the analysis for the system dynamics. Generally, with large control errors, the reconstructed topography image will be distorted. In this paper, a novel smart forward and retraced scanning combined imaging method is proposed which successfully overcomes the problem caused by inadequate Z-axis control. This designed method includes two steps, the hysteresis compensation step in horizontal direction, and the forward and retraced combination imaging step.

Hysteresis compensation is one of the research hot topics for piezo-scanner. Current control-based methods can be classified as feedback control and feedforward control. In the aspect of feedback control, an integral resonant control strategy is proposed in [10], and some repetitive learning control [11] and iterative learning control strategies [12] are well designed to deal with hysteresis; as for feedforward control strategy, neural networks are employed in [13] to set up the reverse model of the piezo-scanner, and an image based strategy is shown in [14] to calculate the reverse model. These methods provide effective compensation for the hysteresis distortion; however, due to the limitation of control bandwidth in feedback loop and the accuracy of the reverse model of piezo-scanner, these methods cannot achieve satisfactory performance for fast scanning tasks. In order to obtain topography images without hysteresis distortion for both slow and fast scanning tasks, some post-processing compensation strategy can be employed. Therefore, a data fusion based post-processing compensation method is proposed. The hysteresis circle is measured in advance, and then the topography height values can be calculated from the original distorted topography image.

For an AFM system, the control input for its piezo-scanner in X-axis is usually in triangular form. For most currently utilized AFMs, only forward scanning signals are employed to reconstruct the sample surface topography, while the data from retraced scanning process is only utilized for adjustment. Based on this fact, researchers have designed some superior trajectories for X-axis control input to shorten the retraced scanning time [15]; however, the retraced scanning data is not sufficiently utilized. It is not difficult to see that the retraced process also provides some useful information for surface construction. For those scanning points of the detected sample, where the retraced scanning process achieves better control effect than forward process, more accurate topography image can be constructed from retraced process data. Based on this observation, a forward and retraced combined imaging method is proposed in this paper, which fully utilizes data from both forward and retraced processes to enhance imaging features. This imaging method shows the great advantage of more accurate topography reconstruction, especially for fast scanning tasks,

*This work is supported by National Natural Science Foundation (NNSF) of China (61127006).

and it can be conveniently implemented in existing AFM systems.

The remainder of this paper is organized as follows. In the next section, the basic idea and general scheme for this novel imaging method is stated. Subsequently, the forward and retraced scanning combined imaging method is introduced in detail. Followed are some simulation and experimental results to demonstrate the performance of the imaging method. At last is the conclusion.

2 Basic Idea and General Scheme

For most commonly used AFM systems, the control input for X-axis is in triangular form. When scanning in low speed, the control effects in Z-axis are well enough at most detected points. Therefore, the forward scanning signals are sufficient to calculate the topography height values. However, for fast scanning tasks, because of the control effects degradation, the forward scanning signals are insufficient to reconstruct an accurate topography image. Here now, the retraced scanning signals can perform as remedial measures. It is shown below with an example.

Without considering the hysteresis distortion, the line scanning results of the calibration gratings are shown in the sketch Figure 1. Figure 1 (a) and (b) show the topography and Z-axis control errors for forward scanning respectively, and Figure 1 (c) and (d) show the results for retraced scanning. In segment AB, the control error for forward scanning is much larger than that for retraced scanning; therefore we tend to trust the topography result for retraced scanning much more than that for forward scanning in this segment. Likewise, we tend to adopt the topography result for forward scanning in segment CD.

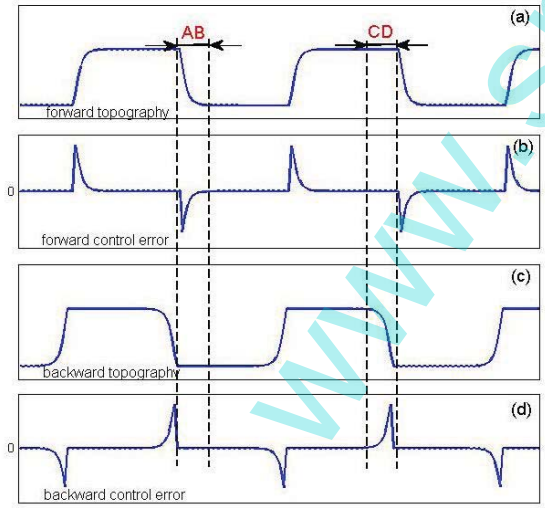

Figure 1. One-line scanning sketch graph: (a) forward scanning topography, (b) forward scanning control error, (c) retraced scanning topography, (d) retraced scanning control error.

In other words, the basic idea is to combine the forward and retraced scanning images, according to the control errors, to calculate the final, more accurate, topography image.

However, due to the hysteresis phenomenon, both the forward and retraced images will be distorted. They will not be consistent with each other. Specifically, as shown in Figure 5 in section 4, in the forward image, the grating will be wider in the left part and narrower in the right part, while the situation will be contrary in the retraced image: narrower in the left part and wider in the right part.

Therefore, before the combination process, the hysteresis distortion needs to be well compensated for both forward and retraced scanning images.

The general scheme of this novel imaging method is shown in Figure 2. Firstly, some specific imaging method, such as static imaging method or piezo-scanner dynamic characteristics considered dynamic imaging method [8], is utilized to obtain the forward and retraced images; then the hysteresis distortion is compensated in both images; with enough consistence, the novel combination strategy will be employed to calculate the final accurate topography image.

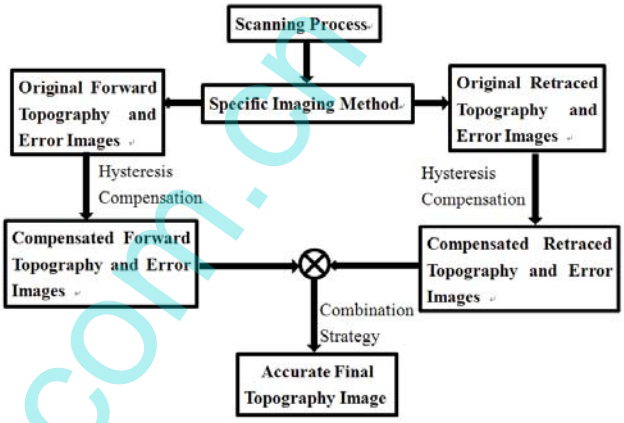

Figure 2. General scheme for the forward and retraced scanning combined imaging method.

3 Forward and Retraced Combined Imaging Method

3.1 Data Fusion Based Hysteresis Compensation

For the brevity of description, only X-axis hysteresis compensation is considered to clarify the compensation strategy, and the discussion is also valid for Y-axis. This proposed data fusion based hysteresis compensation strategy is a post-processing method.

When the X-axis control input for the piezo-scanner is the commonly used triangular form, the hysteresis circle for an exact scanning frequency is shown in Figure 3, the lower curve presents for forward scanning and the upper curve presents for retraced scanning. With the actuation voltage increased/decreased, the displacement varies nonlinearly, therefore, the reconstructed topography is distorted.

In order to compensate the distortion, the hysteresis circle is measured in advance with high-bandwidth position sensors in several considered frequencies as 5Hz, 10Hz, 20Hz, 50Hz, etc. Then the maximum displacement $s_{\max}$ is equally divided as $s_1, s_2, ..., s_q, ..., s_N$ where N is the resolution for the reconstructed topography image, which is shown in Figure 3. For the displacement s_q, we can find the ideal control input u_x in forward scanning process and the ideal control input u_y in retraced scanning process. The control input is discrete in reality, therefore the control input u_x and u_y are always between two real control inputs, as

here u_x is between u_a and u_{a+1}, u_y is between u_b and u_{b+1}. Now the task is to find out the topography heights for X-axis control input u_x in forward scanning and u_y in retraced scanning. As the situations are similar, here only the control input u_x is considered. The topography height signals for X-axis control inputs, which are near to u_x, can be calculated by some specific imaging algorithms [8, 9]. As a general scheme, it doesn't matter which imaging method is employed. In order to show its universality, here the commonly used imaging formula is employed as:

$$h_k = k_s U_k \tag{1}$$

where h_k is the topography height for X-axis control input u_k, U_k is the control input in Z-axis of the piezo-scanner for X-axis control input u_k, and k_s is the static gain between the control input and the piezo-scanner displacement in Z-axis. Then the topography height h_x for the X-axis control input u_x can be calculated as:

$$h_x = \sum_{i\in\Omega_1} \alpha_i h_i \tag{2}$$

where Ω_1 is the neighboring point set around u_x, and α_i is the weight coefficient satisfies:

$$\sum_{i\in\Omega_1} \alpha_i = 1 \tag{3}$$

Now the task is to determine the neighboring point set Ω_1 and the weight coefficient α_i.

Here the neighboring point set Ω_1 is chosen as several points near to u_x on the same line. For the experiment results shown below, if u_x is between two points u_a and u_{a+1}, then the two points a and $a+1$ are chosen as Ω_1; if u_x is on one point u_a exactly right, then $a-1$, a, and $a+1$ are chosen as Ω_1.

For X-axis control input u_k, the control error in Z-axis, which is the difference between the setpoint and the laser detection system feedback signal, is noted as e_k. Then the confidence level value for h_k is defined as:

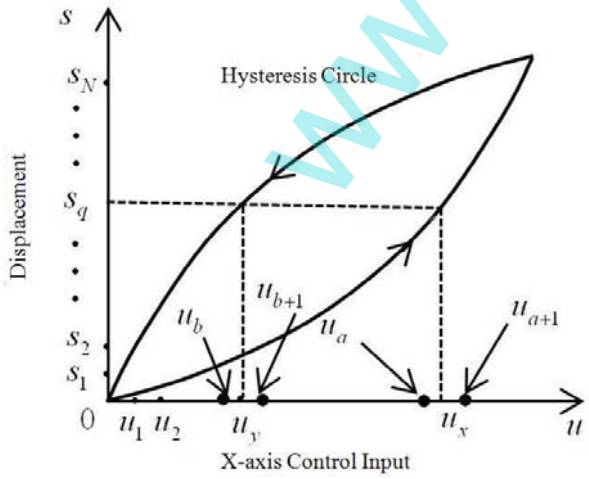

Figure 3. Hysteresis circle for piezo-scanner

$$\lambda_k = \exp\left(\frac{-|e_k|}{3\sigma}\right) \tag{4}$$

where σ is the standard deviation of all the control errors in Z-axis.

Then the weight coefficient α_i can be defined as:

$$\alpha_i = \frac{\lambda_i \beta_i}{\sum_{j\in\Omega_1} \lambda_j \beta_j} \tag{5}$$

where β_j is the forgetting factor defined as:

$$\beta_j = \frac{1}{\theta_1 + \left(\frac{u_j - u_x}{\Delta u}\right)^2} \tag{6}$$

where Δu is the X-axis actuation voltage increment unit such as $u_{a+1} - u_a$; θ_1 is a small positive value to avoid singularity, which is chosen 0.1 in the experiment results shown below.

Therefore, a compensated topography image can be obtained from Equation 2. With the high bandwidth and high accuracy position sensors, the hysteresis circle of the piezo-scanner in high speed scanning process can be well measured, and then the hysteresis distortion even in high speed imaging process can be effectively compensated.

With the above compensation, two new topography images can be obtained, one is for forward scanning, the other is for retraced scanning. Preparing for the next step, forward and retraced scanning combination, the newly control error images need to be calculated as:

$$e_x = \sum_{i\in\Omega_1} \alpha_i e_i \tag{7}$$

where e_x is the control error in Z-axis at the point s_q, corresponding to X-axis control input u_x. This equation is similar with Equation 2.

The same compensation strategy is also applied to Y-axis, and then two hysteresis compensated topography images and two hysteresis compensated control error images are obtained, and they are consistent with each other point by point.

3.2 The Combination Strategy

After the hysteresis compensation, the topography image for forward scanning is noted as I_f, the control error image for forward scanning is noted as E_f, for retraced scanning, the images are noted as I_r and E_r, the final calculated topography image is noted as I_{final}. The notation $I_f(i,j)$ means the value at the point (i,j) in image I_f, and it is similar for $I_r(i,j)$, $E_f(i,j)$, $E_r(i,j)$, and $I_{final}(i,j)$.

The final topography image I_{final} can be calculated as:

$$I_{final}(i,j) = \sum_{(p,q)\in\Omega_2} I_f(p,q)\gamma_f(p,q) + \sum_{(p,q)\in\Omega_2} I_r(p,q)\gamma_r(p,q) \tag{8}$$

Where Ω_2 is the neighboring point set around point (i,j), $\gamma_f(p,q)$ is the weight coefficient at point (p,q) for

forward scanning and $\gamma_r(p,q)$ is similar for retraced scanning. The weight coefficients satisfy:

$$\sum_{(p,q)\in\Omega_2}\gamma_f(p,q)+\sum_{(p,q)\in\Omega_2}\gamma_r(p,q)=1 \tag{9}$$

For smooth sample surface, Ω_2 is proper to choose as several points around (i,j). In the simulation and experiments for this paper, Ω_2 is chosen as 9 points: $(i-1,j-1)$, $(i-1,j)$, $(i-1,j+1)$, $(i,j-1)$, (i,j), $(i,j+1)$, $(i+1,j-1)$, $(i+1,j)$, and $(i+1,j+1)$.

Similarly as in the previous section, confidence level values for the points in topography images are defined as:

$$\eta_f(i,j)=\exp\left(\frac{-|E_f(i,j)|}{3\sigma_f}\right) \tag{10}$$

$$\eta_r(i,j)=\exp\left(\frac{-|E_r(i,j)|}{3\sigma_r}\right) \tag{11}$$

Here $\eta_f(i,j)$ and $\eta_r(i,j)$ are the confidence level values for the point (i,j) in I_f and I_r respectively, and σ_f, σ_r are the standard deviations of the Z-axis control errors in E_f and E_r respectively.

Therefore the weight coefficients $\gamma_f(p,q)$ and $\gamma_r(p,q)$ in Equation 8 can be calculated as:

$$\gamma_f(p,q)=\frac{\eta_f(p,q)\xi(p,q)}{\sum_{(p',q')\in\Omega_2}\eta_f(p',q')\xi(p',q')} \tag{12}$$

$$\gamma_r(p,q)=\frac{\eta_r(p,q)\xi(p,q)}{\sum_{(p',q')\in\Omega_2}\eta_r(p',q')\xi(p',q')} \tag{13}$$

where $\xi(p,q)$ is the forgetting factor:

$$\xi(p,q)=\frac{1}{\theta_2+(p-i)^2+(q-j)^2} \tag{14}$$

Here θ_2 is chosen as 0.5 to avoid singularity, i and j are the same as in Equation 8.

Finally, the forward and retraced scanning combined topography image can be calculated from Equation 8.

4 Simulation and Experimental Results

To verify the validity of the proposed forward and retraced scanning combined imaging method, simulations are firstly taken in a virtual AFM system [16]. The contact mode is chosen to implement the simulation tests. The simulation aims to show the effect of the combination step, so the hysteresis compensation step is not considered here, which will be considered in the following experimental results.

The model and parameters of a practical AFM system are adopted to implement the illustrative study. That is, a 3rd order model is utilized to describe the Z-axis dynamics of the piezo-scanner:

$$G(s)=\frac{6.283\times10^4 s^2+1.935\times10^7 s+1.168\times10^{13}}{s^3+6.306\times10^4 s^2+1.837\times10^8 s+1.1063\times10^{13}} \tag{15}$$

and the voltage amplifier and position sensor detector sensitivity are chosen as 16 and 9.7×10^{-9} nm/V [8]. For the other parameters, please refer to [16].

Calibration grating is one of the commonly used testing samples because of its tough surface topography. For the simulation, square samples with height of 12nm and frequency of 10Hz and 50Hz are utilized as the virtual samples. The simulation results are shown in Figure 4.

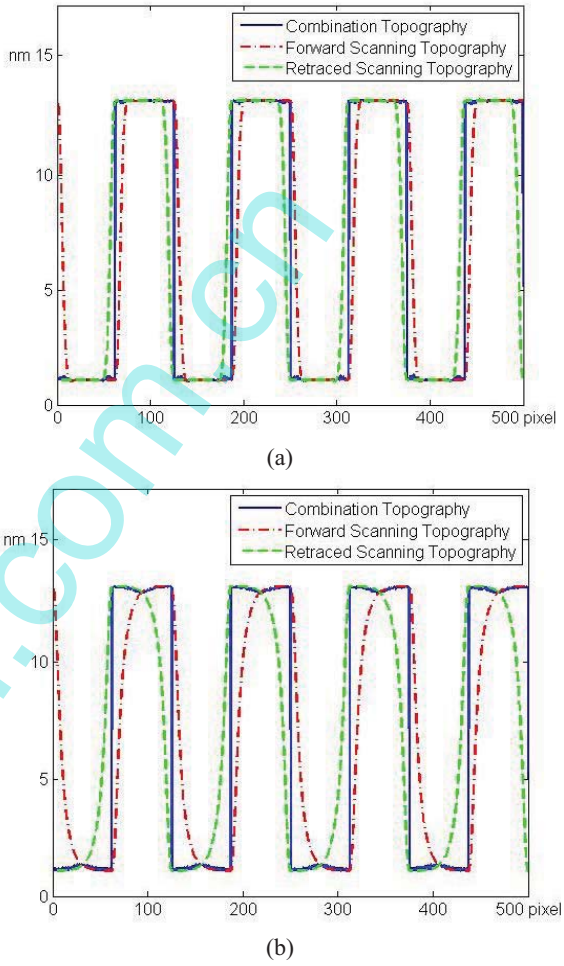

Figure 4. Calibration grating scanning simulation results: (a) 10Hz scanning results; (b) 50Hz scanning results.

It is shown in Figure 4 that the combination imaging method provides a much better performance especially for fast scanning tasks. In Figure 4(b), a little distortion, sunken phenomenon, appears on the steps. This is because of the control effects degradation for both forward and retraced scanning process. This similar distortion also appears in the experimental results in Figure 6(b).

To further demonstrate the performance of the proposed forward and retraced combined imaging method, some experiments are conducted on an AFM system. This system is composed of four parts: a commercial AFM apparatus (CSPM 4000, Being-Nano Inc., P.R. China), high-performance cantilevers (CSC21/Cr-Au, μ Masch Inc., USA), a self-developed RT-Linux based real-time control platform [17], and an additional high-quality capacitive displacement sensor (ADE MicroSence 8810). The control period for this system is set as 50 μs, equivalent to a wide control bandwidth of 20Khz. Proportional-integral (PI)

control strategy is utilized for Z-axis feedback control. The capacitive displacement sensor has a high bandwidth of 10Khz and an accuracy of 0.01nm, which is capable to obtain the hysteresis circle even in fast scanning speed as 50Hz line frequency. The scanning sample is a calibration grating (μ Masch Inc., USA) with nominal height of 84nm ± 1.5nm and period of 3 μm . The experiments are taken in contact mode. In fact, it is easy to find out that this imaging method is suitable for taping mode too.

Firstly, the hysteresis compensation results will be shown. The sample is scanned at the speed of 20Hz, and 50Hz line frequency, respectively, with the scanning scope set as 10 μm × 10 μm , and the image resolution as 400 × 400 pixels. The one-line topography results are shown in Figure 5.

As in Figure 5(a), segment B means the same part in (1'), (2'), (3') and (4'), however, in (1') and (2'), before hysteresis compensation, segment B is obviously not consistent with

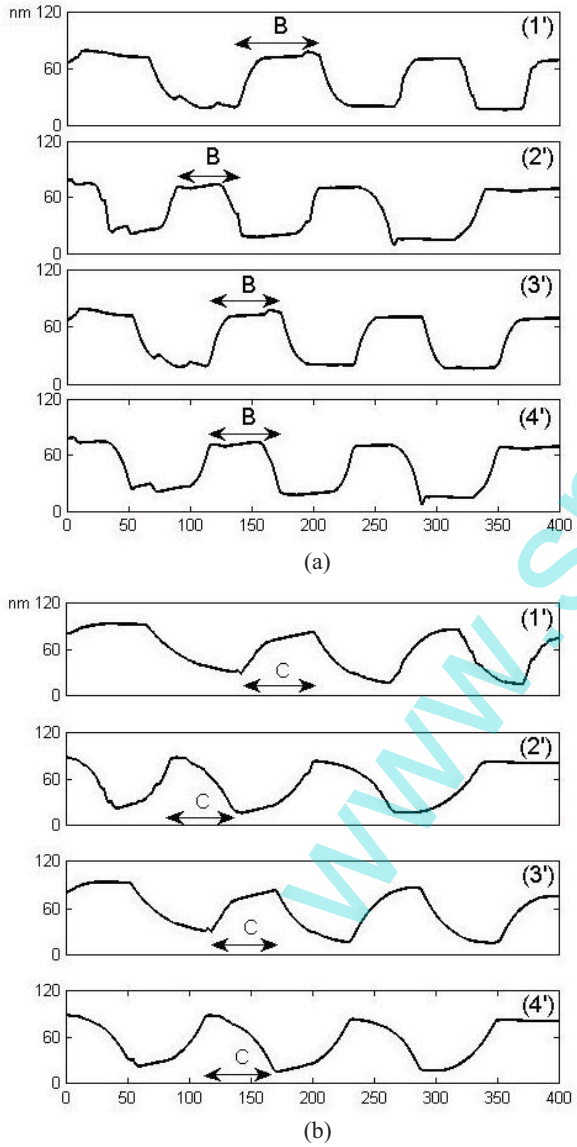

Figure 5. One-line topography experimental results: (a) 20Hz (b) 50Hz; in each subfigure: (1') and (3') present the forward scanning topography before and after hysteresis compensation respectively, (2') and (4') present retraced scanning topography before and after hysteresis compensation respectively. The sgements B, C mean the same part in each subfigure.

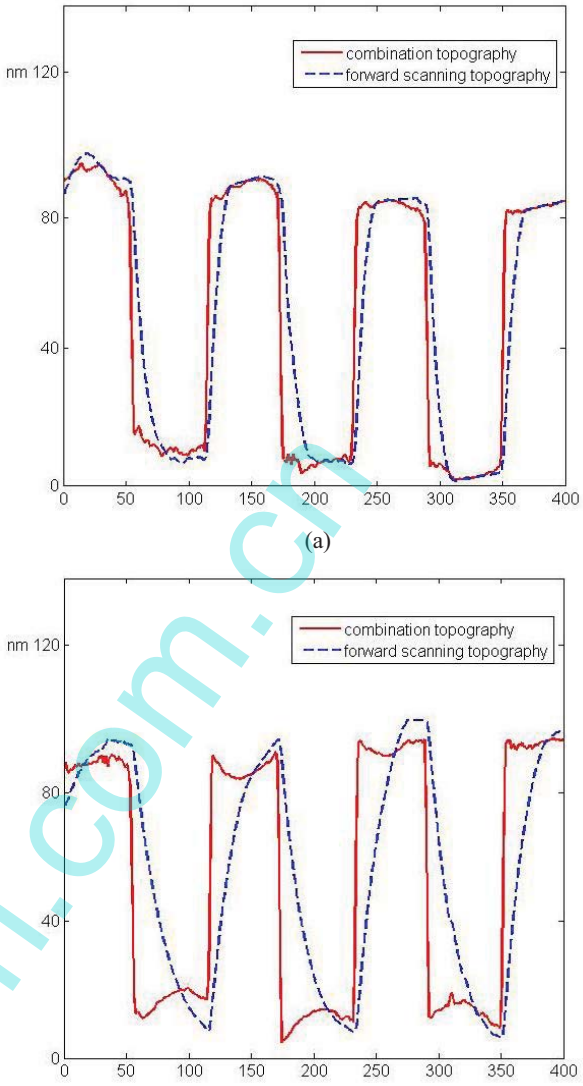

Figure 6. Calibration grating scanning results comparison between the combination topography and the forward scanning topography: (a) 20Hz, (b) 50Hz.

each other. Meanwhile, in (3') and (4'), the segment B is well aligned. The same situation appears in Figure 5(b) with segment C. Therefore, the hysteresis distortion has been effectively compensated even in fast scanning speed, and after the compensation, the forward topography line has been satisfactorily consistent with the line retraced, therefore it has reached a basis for the next step.

In Figure 6, the forward and retraced topography combination results are shown. The scanning speed is also 20Hz, and 50Hz line frequency, respectively. From the one-line topography, we can see that, at the up-edges and down-edges of the grating, the combined final topography line is obviously consistent with the actual calibration grating much better, especially for fast scanning speed shown in Figure 6(b). As in Figure 6(b), because of the high scanning speed of 50Hz, the original forward and retraced scan lines are both distorted seriously; therefore the combined line shows some distortion as in the midst of the grating steps, which is similar as in Figure 4(b). Delightfully, it still shows much improvement for the proposed combined imaging method.

Figure 7 shows the comparison between the forward scanning topography image and the combined method topography image for 50Hz line frequency. Because of the slowly ascending character at the grating edges as shown in Figure 6(b), the forward scanning image Figure 7(a) seems blurry, and Figure 7(b) is consistent with reality much better.

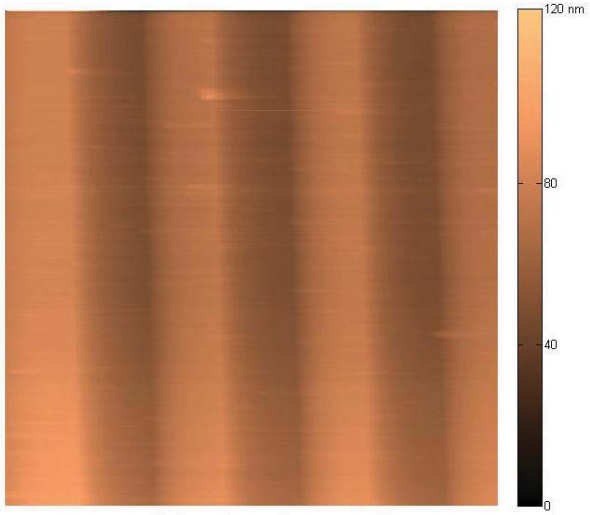

(a) Forward scanning topography

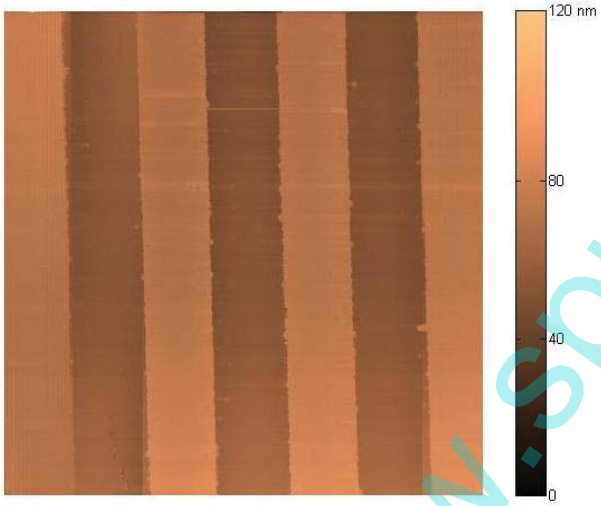

(b) Combination topography

Figure 7. Calibration grating topography image comparison for 50Hz line frequency: (a) forward scanning topography, (b) combination topography.

5 Conclusion

In this paper, a forward and retraced scanning combined imaging method for atomic force microscopy is proposed to enhance its imaging performance especially for fast scanning tasks. This imaging method includes two steps, the first one is a data fusion based post-processing hysteresis compensation, which reaches a basis for the second step. In the second step, the forward and retraced scanning topographies are combined together to calculate the final accurate sample surface topography. The efficacy of the proposed imaging method is verified by the simulation and experimental results of scanning calibration gratings at different speeds. It is shown that this imaging method has markedly enhanced the imaging performance.

References

[1] G. K. Binnig, C. F. Quate, and C. Gerber, Atomic force microscope, *Physical Review Letters*, vol. 56, pp. 930-933, March 3 1986.

[2] G. Mangamma, S. Dash, and A.K. Tyagi, AFM investigations on N+ implanted TiN, IEEE Transactions on Nanotechnology, vol. 12, no. 6, pp. 1007-1011, 2013.

[3] A. J. Fleming, Dual-stage vertical feedback for high-speed scanning probe microscopy, *IEEE Transactions on Control Systems Technology*, vol. 19, no. 1, pp. 156-165, 2010.

[4] B.J. Kenton and K.K. Leang, Design and Control of a Three Axis Serial Kinematic High Bandwidth Nanopositioner, *IEEE/ASME Transactions on Mechatronics*, vol. 17, no. 2, pp. 356-369, April 2012.

[5] Y. Zhang, Y. Fang, J. Yu, and X Dong, Note: A novel atomic force microscope fast imaging approach: Variable-speed scanning, *Review of Scientific Instruments*, vol. 82, no. 5, p. 056103(2011).

[6] Y. Fang, Y. Zhang, N. Qi, and X. Dong, AM-AFM Systems Analysis and Output Feedback Control Design with Sensor Saturation, *IEEE Transactions on Nanotechnology*, vo. 12. no. 2, pp. 190-202, 2013.

[7] M.S. Rana, H.R. Pota, and I.R. Petersen, High-Speed AFM Image Scanning Using Observer-Based MPC-Notch Control, *IEEE Transactions on Nanotechnology*, vol. 12, no. 2, pp. 246-254, 2013.

[8] X. Ren, Y. Fang, N. Qi, M. Wu, X. Feng, A Practical Dynamic Imaging Method for Fast Scanning AFMs, *Instrumentation Science and Technology*, vol. 41, iss. 4, pp. 394-405, July 2013.

[9] S. Kuiper, P. Van den Hof, and G. Schitter, Towards Integrated Design of a Robust Feedback Controller and Topography Estimator for Atomic Force Microscopy, in *Proceedings of the 18th IFAC World Congress,* Milan, Italy, 2011, pp. 12709-12714.

[10] B. Bhikkaji, Y.K. Yong, I.A. Mahmood, S.O.R. Moheimani. Diagonal Control Design for Atomic Force Microscope Piezoelectric Tube Nanopositioners, *Review of Scientific Instruments*, 2013, 84(2): 023705.

[11] Y. Zhang, Y. Fang, X. Dong, X. Zhou. A Novel Learning Control Strategy for Hysteresis and Vibration of Piezo-Scanners, in *proc. 48th IEEE Conf. Decision and Control, and the 28th Chinese Control Conference*, 2009, Shanghai, P.R. China, Dec. 16-18,2009, pp. 750-755.

[12] K.S. Kim, and Q. Zou, A model-free inversion-based iterative feedforward control for precision output tracking of linear time-invariant systems, *IEEE/ASME Transactions on Mechatronics*, to appear.

[13] X. Zhao, Y. Tan. Modeling Hysteresis and Its Inverse Model Using Neural Networks Based on Expanded Input Space Method, *IEEE Transactions on Control Systems Technology*, 2008, 16(3): 484-490.

[14] Y. Zhang, Y. Fang, X. Zhou, et al. Image-based Hysteresis Modeling and Compensation for an AFM Piezo-scanner, *Asian Journal of Control*, 2009, 11(2): 166-174.

[15] A.J. Fleming and A.G. Wills, Optimal Periodic Trajectories for Band-Limited Systems, *IEEE Transactions on Control Systems Technology*, 2009, 17(3): 552-562.

[16] X. Zhou, Y. Fang, A Virtual Tapping-Mode Atomic Force Microscope, in *Proc. 1st IEEE International Conf. Nano/Micro Engineered and Molecular Systems*, pp. 501-504, Zhuhai, China, January 2006.

[17] X. Zhou, Y. Fang, X. Dong, Y. Zhang, Real-time Feedback Control System for AFM Based on RTLinux, *Computer Engineering*, 34(15): 226-228, 2008.